Arch. Metall. Mater. **71** (2026), 2, 465-471

DOI: https://doi.org/10.24425/amm.2026.158825

DIMKA I. FACHIKOVA[1*], TSVETELINA L. LIUBENOVA[1]

SEM AND EDX STUDY OF ZINC-MAGNESIUM PHOSPHATE COATINGS ON MILD STEEL SURFACES

The work presents results of the formation, composition, structure and corrosion resistance of phosphate coatings on mild steel surfaces, obtained in zinc-magnesium phosphating solutions. The mass/thickness of the coating has been measured by means of gravimetric technique under the following conditions: concentration of the working solutions 5, 10, 15 and 20 vol.%; duration of the process 5, 10, 15 and 20 min; temperature 20, 40, 60 and 80°C. The elements that make up the coatings are determined by EDX analysis. The morphology and topography of the coatings are investigated by scanning electron microscopy (SEM). Potentiodynamic polarization measurement was used to determine the corrosion resistance and protective ability of the coatings.

Keywords: Magnesium phosphating; zinc phosphating; mild steel; conversion coatings; tin films; corrosion resistance

1. Introduction

Phosphating is a chemical treatment applied to metal surface that creates a thin adhering conversion films of phosphates as a sublayer for subsequent polymeric coatings or painting, a lubrication under the condition of deep drawing processes or to improve corrosion resistance [1-5].

The most common type in practice is zinc phosphating. The modifying of zinc baths by some additives such as Cu^{2+}, Ni^{2+}, Mn^{2+}, Ca^{2+}, the optimizing pH and temperature of the baths as well as post-sealing and other methods have been used to improve the properties of obtained coatings [6-10].

Magnesium phosphating is a relatively new treatment of metal surfaces, which can replace the traditional and most widely used zinc phosphating. The advantages of using magnesium phosphating preparations included: easy preparation, lower prices compared to other phosphate baths, obtaining coatings with good corrosion resistance and adhesion of subsequent paint and polymer coatings. The magnesium phosphate coating or bication zinc-magnesium phosphate coating has shown slightly better corrosion behavior compared with a zinc phosphate coating. Therefore, developing a novel phosphate coating seems to be necessary [11-19]. Three phosphate layers (zinc-based, zinc/iron-based and manganese-based) were obtained by immersion on C45 steel, followed by depositing a layer of elastomer-based paint. The overall results show that all types of layers increase the corrosion resistance of the steel [20].

In recent years, based on magnesium, biodegradable materials have been widely explored. Designed for medical use, a new experimental Mg-based biodegradable alloy (Mg-Ca with additions of Zn) has been tested in order to control the corrosion rate [22]. Magnesium oxide nanoparticles (MgO NPs) have distinct physicochemical and biological properties, including biocompatibility, biodegradability, high bioactivity, significant antibacterial properties, and good mechanical properties, which make it a good choice as a reinforcement in composites [23].

All the mentioned properties suggest that the new phosphate coating could theoretically be used even as an anti-corrosion surface treatment for bioimplants for bone substitutes made of magnesium alloys.

The aim of the presented work is to determine the parameters of a new zinc-magnesium phosphating bath, as well as to characterize a phosphate coating on steel surfaces by SEM and EDX analyses.

2. Experiment

2.1. Material and samples

In the present work, square steel probes (thickness 1.0 mm and working surface area 5×10^{-3} m^2) were investigated. The chemical composition of steel is taken from the certificate

[1] UNIVERSITY OF CHEMICAL TECHNOLOGY AND METALLURGY, FACULTY OF CHEMICAL TECHNOLOGY, 8 KLIMENT OHRIDSKI BLVD., 1756 SOFIA, BULGARIA

* Corresponding author: dimkaivanova@uctm.edu

of the purchased material (see TABLE 1). The preparation of testing samples includes sequentially: immersion in a mixture of ethanol and diethyl ether and rinsed with deionized water to remove any surface contaminants; pickled in 15% hydrochloric acid + inhibitor at room temperature for 3 min and then rinsed with deionized water; finally, the samples were immersed in the phosphating bath.

The electrochemical experiments were carried out with plate-shaped specimens with dimensions accordance with ISO 17475:2005 and a fixed working surface area of 1×10^{-4} m^2. In addition, square plate samples (1×10^{-3} m^2) were used in case of all physical methods applied.

TABLE 1

The chemical composition of steel (in wt.%)

C	Mn	Si	P	S	Cr	Ni	Cu	Fe
0.17	0.36	0.016	0.01	0.029	0.06	0.06	0.11	bal.

2.2. Solutions

The phosphating liquid concentrate contains zinc and magnesium (10%) orthophosphates, phosphoric acid, inorganic activators, stabilizing agents as well as surfactants are added. The ratio P_2O_5:NO^{3-} = 1:3 was used.

The working media are aqueous solutions of the phosphating concentrate in the range of 5.0÷20.0 vol.%. The experiments are carried out at a temperature interval 20÷80°C and a process duration 0.5÷20.0 min. The working/model media used for the corrosion experiments is 0.6 M NaCl.

2.3. Methods

2.3.1. Gravimetric method

The gravimetric method is used to study the kinetics of formation and determine the phosphate coating's mass/thickness growth, depending on the effect of different factors. Its application requires careful measurement of sample mass (in grams) after the phosphating (m_1), as well as its mass after coating removal (m_2). Using the next equation allows determination of the phosphate coating mass/thickness, M:

$$M = \frac{(m_1 - m_2)}{S},\ \text{g m}^{-2}$$

Where S – sample surface area, m^2.

2.3.3. Electrochemical methods

Potentiodynamic polarization method. The polarization curves take down potentiostatically or potentiodynamically allow the determination of various electrochemical and corrosion parameters such as a corrosion rate, corrosion potential, etc. All measurements were performed in a model 0.6M NaCl solution in range of potentials from –0.250 to +0.300 V (vs. OCP) and a scan rate 5 mV s^{-1}.

2.3.4. Physical methods

Scanning electron microscopy (SEM). The morphology and structure of the coatings were examined by scanning electron microscopy, using a SEM/FIB LYRA I XMU, TESCAN electron microscope, equipped with ultrahigh-resolution scanning system secondary electron image (SEI).

Energy dispersive X-ray spectroscopy (EDX). The energy dispersive spectroscopy is a local X-ray spectral analysis that permits qualitative and quantitative determination of surface micro-volume contents of the order of several μm^3. Apparatus Quantax 200, BRUKER with spectroscopic resolution at Mn-Ka and 1 kcps 126 eV is used.

3. Results and discussion

TABLE 2 presents the values of the most important indicators characterizing the phosphating concentrate: density, ρ; pH; conductivity, σ; total, K_{ta} and free, K_{fa} acidity.

TABLE 2

Characteristics of the phosphating concentrate

Solution	ρ [g cm^{-3}]	pH	σ [mS cm^{-1}]	K_{ta}	K_{fa}
Zn, MgPh	1.32	0.36	89.3	276	48

3.1. Gravimetric measurements

Gravimetric method was used to reveal the effect of the operating conditions (concentration and temperature of the phosphating solutions) as well process duration on the coating thickness, M. The values of the concentration and temperature were selected experimentally.

Typical thickness kinetic plot (M as a function of time) shown in Fig. 1 corresponds to coatings obtained in working solutions at different concentrations (a/ 5.0 vol.%; b/ 10.0 vol.%; c/ 15.0 vol.%; and d/ 20.0 vol.%) and temperatures (20, 40, 60, 80°C) of the phosphating baths, on mild steel surfaces. Coatings with the smallest thickness for all concentrations of the phosphating solutions were obtained at lower temperatures of the phosphating baths –20°C and 40°C, while the largest ones are formed at 60°C and 80°C. At the highest temperature applied in the experiments (80°C), however, a slight decrease in coating thickness was observed compared to that obtained at 60°C.

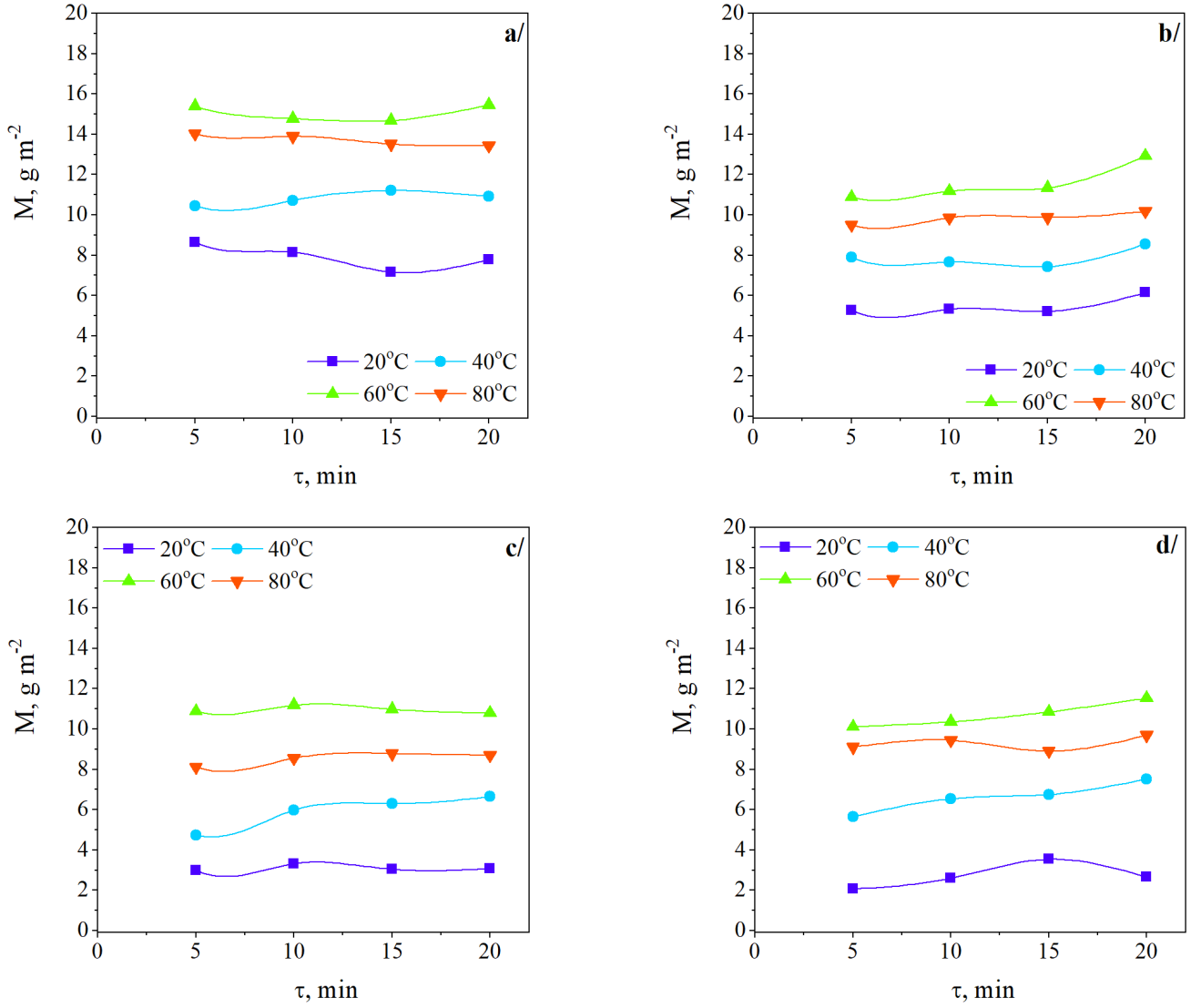

Fig. 1. Influence of the phosphating time τ, on the thickness of the resulting phosphate coatings, M_1: a/ 5.0 vol.%; b/ 10.0 vol.%; c/ 15.0 vol.%; d/ 20.0 vol.%

3.2. SEM analysis

Microphotographs of the phosphating coatings formed on mild steel surfaces are shown in Fig. 2: duration of the process 12 min; working concentration 15.0 vol.%; at temperatures 20°C, 40°C, 60°C and 80°C. At all conditions of coating formation, the sample surfaces are covered almost homogeneously with dense fine films, and the reproducibility of the process is satisfactory high. It follows from the figures that the habit of coatings is constant – i.e. the crystals initiate from one center and increase radially. An exception is the coating obtained at 20°C, where the characteristic crystals are not present on the surface.

The crystals formed from the solution with 40°C are bigger than the other ones – the size of the crystals is about 100 μm. The crystals formed at other temperatures (60°C and 80°C) of the phosphate solution have length between 50 and 100 μm. With increasing the concentration of the phosphating baths, the crystals sizes reduce.

3.3. EDS analysis and distribution of the elements

The main elements containing the phosphate coatings formed on the surface of steel, determined by EDX analysis, are presented in TABLE 3. The registered elements in the coatings (in At.%), obtained at different temperatures of the phosphating solutions and under the same other conditions, are O, P, Fe, Zn and Mg.

The amounts of the registered elements in the coating obtained at 20°C differ significantly. Probably (as is visible from the morphology of the coating in the SEM analysis) under these conditions no crystal formations. The surface looks like it's etched.

In the coatings obtained at the other three temperatures, the amount of oxygen decreases, albeit slightly, with rising working temperature. The amount of iron grows with temperature, while the amounts of phosphorus and zinc remain relatively the same.

Magnesium was detected only in the coatings obtained at 60 and 80°C, with a higher concentration at the former temperature.

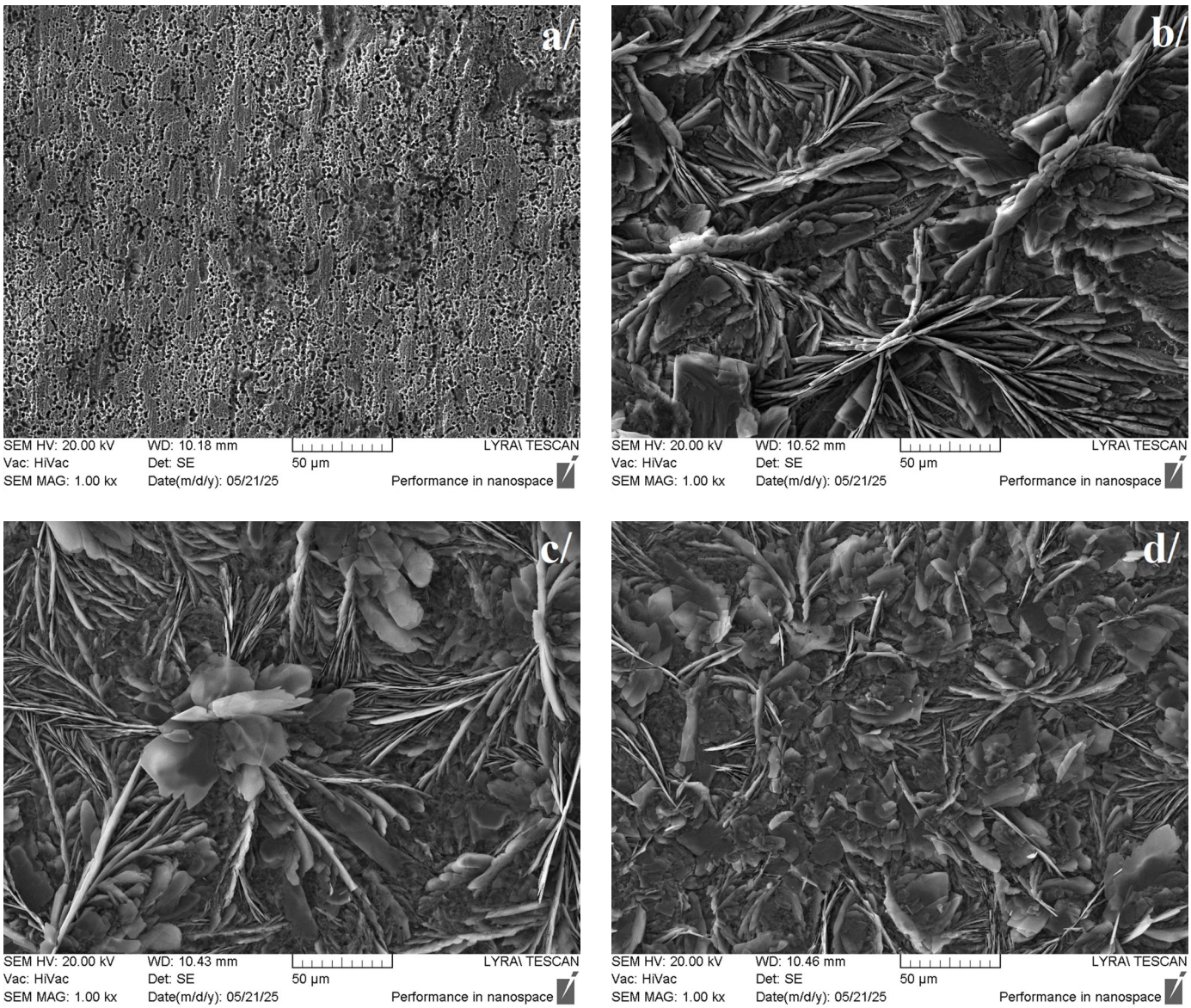

Fig. 2. Microphotographs of thin phosphate coatings obtained in baths of various temperatures: a/ 20.0°C; b/ 40.0°C; c/ 60.0°C; d/ 80.0°C

TABLE 3

Elemental contents of conversion phosphate coatings obtained upon various experimental conditions –20.0÷80.0°C, 12 min and 15.0 vol.%

Elements	20.0°C	40.0°C	60.0°C	80.0°C
	At.%	At.%	At.%	At.%
O	10.92	53.75	49.55	47.86
P	0.07	11.65	11.52	11.30
Fe	88.42	16.41	22.15	24.01
Zn	0.58	18.19	15.35	15.55
Mg	—	—	1.44	1.29
Total:	100	100	100	100

Probably, at 20 and 40°C Mg was not detected due to its very low presence in the coatings.

Fig. 3 presents the distribution of elements on the surface of the phosphate coatings depending on the bath temperature, with magnification being the same to that in the SEM analyses (×1000). In the coating obtained at 20°C (see Fig. 3a), the presence of Fe and very small amount of Zn, O and P predominate, which indicates that practically no crystalline phosphate coating was obtained. In the other coatings obtained at different temperature, the elements are evenly distributed over the surface, which confirms the homogeneity of the phosphate coatings.

3.4. Polarization measurements

The polarization measurements were performed with 4 phosphating specimens and uncoated one for comparison. The coatings were formed at different temperatures (20.0÷80.0°C) in a 15.0 vol.% solutions, for 12 minutes. The conditions were selected from the gravimetric studies taking into account the reproducibility and mass/thickness of the obtained coatings. All measurements were performed in a corrosion model media – 0.6 M NaCl.

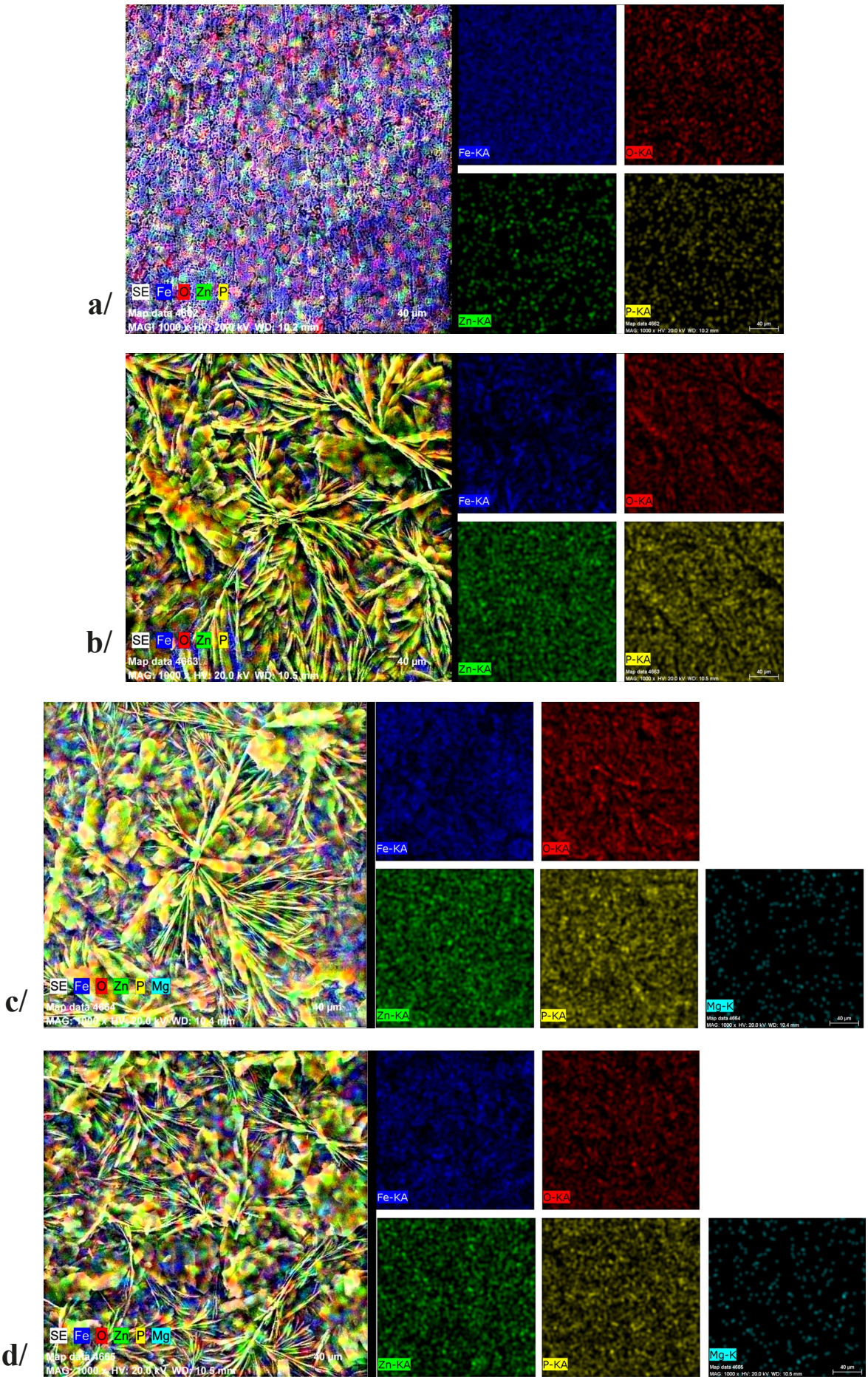

Fig. 3. Distributions of the elements in the phosphate coatings obtained in baths of various temperatures: a/ 20.0°C; b/ 40.0°C; c/ 60.0°C; d/ 80.0°C

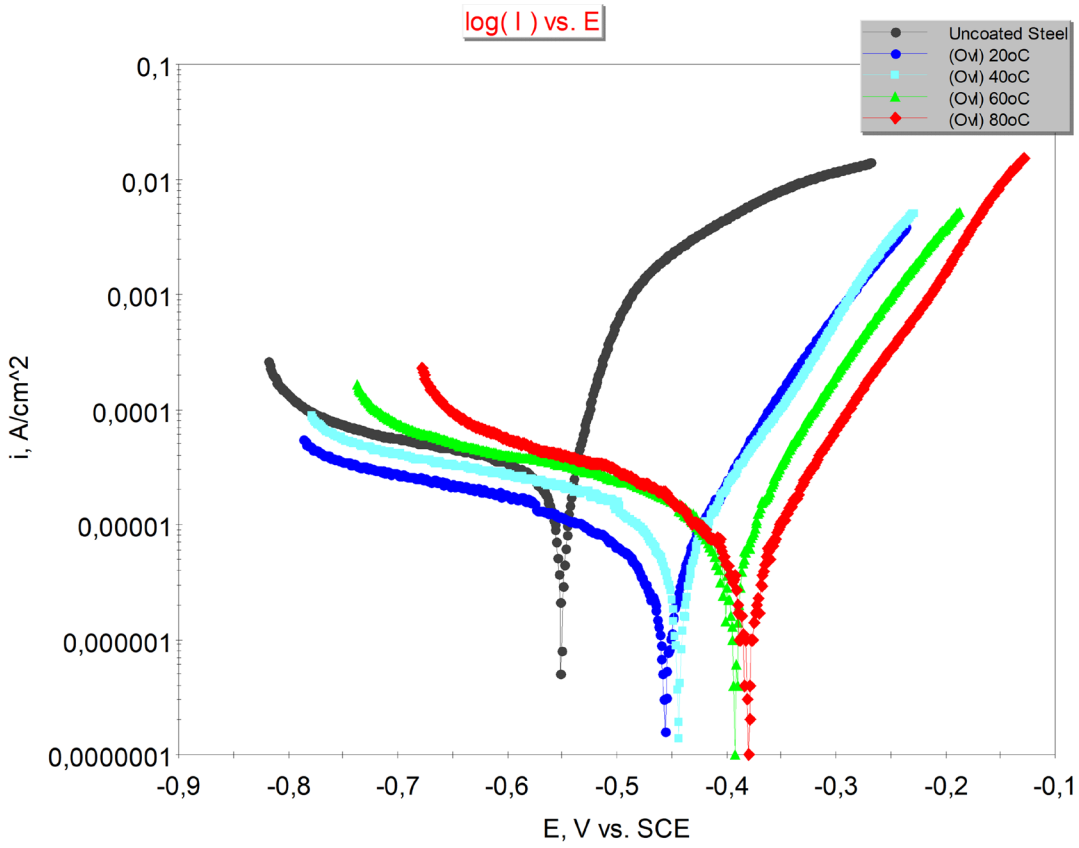

Fig. 4. Potentiodynamic polarization relationships of phosphated specimens taken at room temperature in 0.6 M NaCl, in the potential range from –0.250 to +0.300 V (vs. OCP) and a potential scan rate 5 mV s^{-1}

From the polarization dependencies *"Potential, V (vs. SCE) – Current Density, A* cm^{-2}*"*, presented in Fig. 4, it is seen that there is no substantial difference in their course.

From these dependencies are determined both the corrosion potential and a corresponding current density (see data summarized in TABLE 4). The potential of the phosphated samples is about 100-150 mV more positive than the potential of the uncoated mild steel sample. The more positive potentials and the lower values of the current density of the coated samples show better corrosion resistances vs. uncoated steel.

TABLE 4

Data corresponding to the polarization curves (see Fig. 4)

Sample	E_{corr}, V vs. SCE	i_{corr}, A cm^{-2}
Uncoated Steel	–0.550	0.2×10^{-5}
20°C	–0.460	2.7×10^{-6}
40°C	–0.440	1.9×10^{-6}
60°C	–0.385	1.3×10^{-6}
80°C	–0.370	0.5×10^{-6}

4. Conclusions

The mass/thickness, chemical composition and morphology of phosphate coatings, formed on mild steel in solutions containing zinc and magnesium (10%) orthophosphates, phosphoric acid, inorganic activators, stabilizing agents and surfactants have been determined by gravimetric and electrochemical methods, SEM and EDX. The main results can be outlined as:

1. Coatings with the smallest thickness for all concentrations of the phosphating solutions are obtained at lower temperatures of the phosphating baths – 20°C and 40°C, while the largest ones are formed at 60°C and at 80°C.
2. By SEM observations has been established that at all conditions sample surfaces are covered almost homogeneously with dense and fine phosphating crystal films. An exception is the coating obtained at 20°C, where the crystals are not present on the surface.
3. By EDX analysis the elements in the coatings are registered – O, P, Fe, Zn and Mg (in At.%). Mg was not detected in the coatings obtained at 20 and 40°C, due to its very low presence.
4. From the electrochemical polarizations relationships are determined both a corrosion potential and a current density. The more positive potentials and the lower values of the current density of the coated samples show better corrosion resistances vs. uncoated steel.

Acknowledgments

This research is supported by the Bulgarian Ministry of Education and Science under the National Program "Young Scientists and Postdoctoral Students-2".

REFERENCE

[1] D.B. Freeman, Phosphating and Metal Pre-Treatment: A Guide to Modern Processes and Practice. Woodhead-Foulkner, Cambridge, (1986). ISBN 13: 9780859412995

[12] W. Rausch, The Phosphating of Metals. Finishing Publications Ltd., Teddington, Middlesex, England, (1990). ISBN 0-904477-11-8

[3] P.M. Martin, Handbook of Deposition Technologies for Films and Coatings. 3rd ed.; Elsevier: Amsterdam, The Netherlands, (2010).

[4] U. B. Nair, Special Types of Phosphating – A Review. Corrosion Reviews **13** (1), 17-28 (1995).
DOI: https://doi.org/10.1515/corrrev.1995.13.1.17

[5] T.S.N. Sankara Narayanan, Surface pretreatment by phosphate conversion coatings – A review. Rev. Adv. Mater. Sci. **9**, 130-177 (2005).

[6] M. Fouladi, A. Amadeh, Comparative study between novel magnesium phosphate and traditional zinc phosphate coatings. Materials Letters **98**, 1-4 (2013).
DOI: https://doi.org/10.1016/j.matlet.2013.01.061

[7] D.-P. Burduhos-Nergis, A.V. Sandu, D.-D. Burduhos-Nergis, P. Vizureanu, C. Bejinariu, PhosPhate Conversion Coating – a short review. Arch. Metall. Mater. **68** (3), 1029-103 (2023).
DOI: https://doi.org/10.24425/amm.2023.145471

[8] J. Liu, B. Zhang, W.H. Qi, Y.G. Deng, R.D.K. Misra, Corrosion response of zinc phosphate conversion coating on steel fibers for concrete applications,. Journal of Materials Research and Technology **9** (3), 5912-5921 (2020).
DOI: https://doi.org/10.1016/j.jmrt.2020.03.117

[9] A.-M. Cazac, L.-I. Cioca, P. Lazar, G. Badarau, N. Cimpoesu, D.-P. Burduhos-Nergis, P. Iagaru, R. Cimpoesu, A. Cazac, C. Bejinariu, et al., Effect of Zinc, Magnesium, and Manganese Phosphate Coatings on the Corrosion Behaviour of Steel. Materials **18** (13), 31262025 (2025).
DOI: https://doi.org/10.3390/ma18133126

[10] J. Duszczyk, K. Siuzdak, T. Klimczuk, J. Strychalska-Nowak, A. Zaleska-Medynska, Modified Manganese Phosphate Conversion Coating on Low-Carbon Steel. Materials **13** (6), 1416 (2020).
DOI: https://doi.org/10.3390/ma13061416

[11] J.E. Gray, B. Luan, Protective coatings on magnesium and its alloys – A critical review. J. Alloys Compd. **336** (1-2), 88-113 (2002).
DOI: https://doi.org/10.1016/S0925-8388(01)01899-0

[12] M.F. Morks, Magnesium phosphate treatment for steel. Materials Letters **58** (26), 3316-3319 (2004).
DOI: https://doi.org/10.1016/j.matlet.2004.06.027

[13] T. Ishizaki, I. Shigematsu, N. Saito, Anticorrosive magnesium phosphate coating on AZ31 magnesium alloy. Surf. Coat. Technol. **203** (16), 2288-2291 (2009).
DOI: https://doi.org/10.1016/j.surfcoat.2009.02.026

[14] Li-Yuan Niu, Ji-Xing Lin, Yong Li, Zi-Mu Shi, Lin-Chao Xu, Improvement of anticorrosion and adhesion to magnesium alloy by phosphate coating formed at room temperature. Transactions of Nonferrous Metals Society of China **20** (7), 1356-1360, (2010), DOI: https://doi.org/10.1016/S1003-6326(09)60304-6

[15] M. Fouladi, A. Amadeh, Effect of phosphating time and temperature on microstructure and corrosion behavior of magnesium phosphate coatings. Electrochimica Acta **106**, 1-12 (2013).
DOI: https://doi.org/10.1016/j.electacta.2013.05.041

[16] P. Pokorny, P. Tej, P. Szelag, Discussion about magnesium phosphating. Metalurgija **55** (3), 507-510 (2016). ISSN 0543-5846

[17] S. Yin, H. Yang, Y. Dong et al., Environmentally favorable magnesium phosphate anti-corrosive coating on carbon steel and protective mechanisms. Sci. Rep. **11**, 197 (2021).
DOI: https://doi.org/10.1038/s41598-020-79613-3

[18] N.F. Cirstea, A. Badanoiu, G. Voicu, R.C. Ciocoiu, A.C. Boscornea, Fire Behavior and Adhesion of Magnesium Phosphate Coatings for the Protection of Steel Structures. Appl. Sci. **12**, 12620 (2022).
DOI: https://doi.org/10.3390/app122412620

[19] W. Wang, S. Chen, X. Chen, H. Qian, Y. Zhang, Y. Liu, D. Yan, Anti-corrosion behavior of magnesium phosphate (Mg-P) coatings after exposure to elevated temperatures. Journal of Building Engineering **88**, 109233 (2024).
DOI: https://doi.org/10.1016/j.jobe.2024.109233

[20] D.-P. Burduhos-Nergis, P. Vizureanu, A.V. Sandu, C. Bejinariu, Phosphate Surface Treatment for Improving the Corrosion Resistance of the C45 Carbon Steel Used in Carabiners Manufacturing. Materials **13**, 3410 (2020).
DOI: https://doi.org/10.3390/ma13153410

[21] B. Istrate, C. Munteanu, M.-S. Bălțatu, R. Cimpoeșu, N. Ioanid, Microstructural and Electrochemical Influence of Zn in MgCaZn Biodegradable Alloys. Materials **16**, 2487 (2023).
DOI: https://doi.org/10.3390/ma16062487

[22] A. Saberi, M.S. Baltatu, P. Vizureanu, Recent Advances in Magnesium–Magnesium Oxide Nanoparticle Composites for Biomedical Applications. Bioengineering **11**, 508 (2024).
DOI: https://doi.org/10.3390/bioengineering11050508

[23] A. Saberi, M.-S. Baltatu, P. Vizureanu, The Effectiveness Mechanisms of Carbon Nanotubes (CNTs) as Reinforcements for Magnesium-Based Composites for Biomedical Applications: A Review. Nanomaterials **14**, 756 (2024).
DOI: https://doi.org/10.3390/nano14090756